

Smart Stay Cable Damping — Effects of Sag and Inclination[†]

E.A. Johnson

Dept. of Civil and Environmental Engineering, University of Southern California, Los Angeles, CA 90089-2531

R.E. Christenson & B.F. Spencer Jr.

Dept. of Civil Engineering and Geological Sciences, University of Notre Dame, Notre Dame, IN 46556-0767

Keywords: smart damping, cable galloping, rain-wind induced vibration, cable sag, structural control

ABSTRACT: Cables, such as are used in cable-stayed bridges and other cable structures, are prone to vibration due to their low inherent damping characteristics. Transversely-attached passive viscous dampers have been implemented on some cables to dampen vibration. However, only minimal damping can be added if the damper attachment point is close to the end of the cable. For long cables, passive dampers may provide insufficient supplemental damping to eliminate vibration problems. A recent study by the authors demonstrated that “smart” semiactive damping can provide significantly superior supplemental damping for a cable modeled as a taut string. This paper extends the previous work by adding sag, inclination, and axial flexibility to the cable model. The equations of motion are given. A new control-oriented model is developed for cables with sag. Passive, active, and smart (semiactive) dampers are incorporated into the model. Cable response is seen to be dramatically reduced by semiactive dampers for a wide range of cable sag and damper location.

1 INTRODUCTION

Cables are efficient structural elements that are used in cable-stayed bridges, suspension bridges and other cable structures. These cables are subject to environmental excitations, such as rain-wind induced vibration, and support excitations. Steel cables are flexible and have low inherent damping, resulting in high susceptibility to vibration. Vibration can result in premature cable or connection failure and/or breakdown of the cable corrosion protection systems, reducing the life of the cable structure (Watson and Stafford, 1988). Additionally, cable vibrations can have a detrimental effect on public confidence in the safety of cable structures.

A number of methods have been proposed to mitigate cable vibration. Tying cables together shortens the cables and is intended to shift the frequencies of the cable out of the range of the excitation. This strategy deteriorates the aesthetics of some cable structures. Changing the surface of the cable to reduce susceptibility to environmental excitations has also been explored, but is impractical for retrofit applications and may increase motion during high winds.

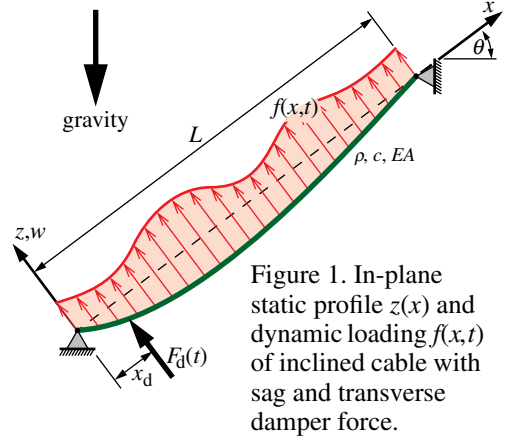
Several researchers (Kovacs, 1982, Sulekh, 1990, Pacheco *et al.*, 1993) have proposed passive control of cables using viscous dampers attached transverse to the cables. They showed that an optimal damper size exists and developed a “universal” design curve to facilitate the design of passive dampers for stay cables. Transverse passive viscous dampers have been applied to the cables on many cable-stayed bridges; however, the damper location is typically restricted to be close to the bridge deck for aesthetic and practical reasons. For longer bridge cables, passive dampers cannot provide enough supplemental damping to eliminate vibration effects without significant changes to the “look” of the structure.

Several recent papers by the authors have shown that semiactive dampers may provide levels of damping far superior to their passive counterparts. Johnson *et al.* (2001) used a taut string model of

[†] An expanded version of this paper will appear in a special “Smart Civil Infrastructure Systems” issue of *Computer-Aided Civil and Infrastructure Engineering* (S.C. Liu, guest editor).

in-plane cable vibration and developed a control-oriented model using a static deflection shape in a series expansion for the cable motion. They showed that a “smart” semiactive damper can provide 50 to 90% reduction in cable response compared to the optimal passive linear damper.

This study extends the aforementioned work to investigate the effects of cable sag, inclination, and axial flexibility on the performance of semiactive cable damping. An extension to the control-oriented model of Johnson *et al.* (2001) is developed herein to accommodate these cable characteristics. Cables with linear passive viscous dampers, active dampers, and smart (semiactive) dampers are examined for various levels of sag and damper location. Semiactive damper performance is seen to degrade some for certain ranges of sag, but far less than their passive counterparts. Semiactive dampers are further shown to perform significantly better than passive dampers for all sag levels typical for stay cables and for most larger levels of sag.



2 IN-PLANE MOTION OF CABLES WITH SAG

2.1 Equations of Motion

Consider the uniform cable suspended between two supports of different heights, as shown in Figure 1. This study investigates cables with a flat profile (flat-sag cables); for a horizontal cable, this requires the sag to span ratio be less than 1:8 (Irvine, 1981). Further, the effects of longitudinal flexibility are included and flexural rigidity is ignored. The static profile of the cable can be approximated by a parabolic curve and the in-plane transverse cable motion $w(x, t)$, relative to the static profile, is given by the nondimensional equation of motion (Irvine, 1981)

$$\ddot{w}(x, t) + c\dot{w}(x, t) - \frac{1}{\pi^2}w''(x, t) + \frac{\lambda^2}{\pi^2}\left[\int_0^1 w(\xi, t)d\xi\right] = f(x, t) + F_d(t)\delta(x - x_d) \quad (1)$$

in the domain $0 \leq x \leq 1$, with boundary conditions $w(0, t) = w(1, t) = 0$. c is the viscous damping per unit length, $(\cdot)'$ and (\cdot) denote partial derivatives with respect to x and t , respectively, $f(x, t)$ is the distributed load on the cable, $F_d(t)$ is a transverse in-plane damper force at location $x = x_d$, and $\delta(\cdot)$ is the Dirac delta function. λ^2 is the nondimensional independent parameter (Irvine, 1981)

$$\lambda^2 = [(\rho g L \cos \theta) / H]^2 [(EAL) / (HL_e)] \quad (2)$$

where ρ is the cable mass per unit length, L is the length of the cable, θ is the inclination angle, H is the component of cable tension in the longitudinal x -direction, EA is the axial cable stiffness, and $L_e = L[1 + (\rho g L \cos \theta)^2 / 8H^2]$ is the static (stretched) length of the cable. The effects of cable sag, angle-of-inclination, and axial stiffness on the nondimensional dynamic response of the system enter only through the independent parameter λ^2 .

Stay cables on cable-stayed bridges typically have λ^2 values on the order of 1 or smaller (Gimsing, 1983). Typical transmission line characteristics (Tunstall, 1997) give a λ^2 in the neighborhood of 90. The main cable on a suspension bridge is generally in [140,350] (Gimsing, 1983). Specific performance examples will be given below for control of cables with some λ^2 values of interest, as well as general trends as λ^2 increases from 0 to 500. Typical static cable profiles are shown to scale in Figure 2 for several λ^2 values. Even for large λ^2 values, such as the $\lambda^2 = 1000$ shown, the midspan sag-to-length ratio is less than the 1:8 required for the flat-sag cable (i.e. parabolic static profile) assumption for horizontal cables (Irvine, 1981).

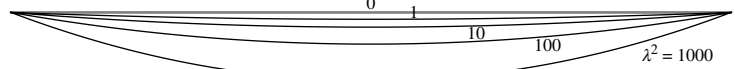


Figure 2. Typical static sag profiles.

2.2 Control-Oriented Series Solution to the Nondimensional Equation of Motion

Determining an accurate and efficient control-oriented design model is the first and fundamental step in the design of a semiactive control strategy. A design model is sought that can capture the salient features of the dynamic system with a relatively small number of degrees-of-freedom (DOFs). Previous transversely-controlled cable models have employed the Galerkin method, using only sine shape functions requiring 350 DOFs, as well as hybrid-type finite element methods which also require numerous DOFs to insure accurate results. Semiactive control design, as well as the computation of performance criteria through simulation with numerous control strategies, is impractical for systems of such size. Thus, successful semiactive control design is dependant on determining a low-order, control-oriented design model. This is accomplished here by including a static deflection shape in addition to the sine series in the approximation of the cable motion.

Using a Galerkin method, the motion of the cable may be computed using a finite series approximation $w(x, t) = \sum_{j=1}^m q_j(t) \phi_j(x)$, where the $q_j(t)$ are generalized displacements and the $\phi_j(x)$ are a set of shape functions that are continuous with piecewise continuous slope and that satisfy the geometric boundary conditions $\phi_j(0) = \phi_j(1) = 0$. A sine series may be used for the shape functions, though Johnson *et al.* (2001) showed that the convergence of this series is slow, making it difficult to construct a control-oriented model. However, they also demonstrated that the introduction of a static deflection shape as an additional shape function significantly improved the series convergence and provided an excellent control-oriented model. This approach is used here as well, though it must be extended to account for sag.

Consider the static deflection of a cable with sag due to a unit load at location $x = x_d$ — the same as the equation of motion (1) without the dynamic terms and with a unit point load on the right hand side. Solving for the static deflection and normalizing gives a static deflection shape function

$$\phi_1(x) = \frac{12 + \lambda^2}{12 + \lambda^2 - 3\lambda^2 x_d(1 - x_d)} \left[\frac{x}{x_d} + \left(1 - \frac{x}{x_d}\right) \frac{H(x - x_d)}{1 - x_d} - \frac{3\lambda^2}{12 + \lambda^2} x(1 - x) \right] \quad (3)$$

where $H(x - x_d)$ is the Heaviside function. As the independent parameter λ^2 tends to zero, (3) reverts to the triangular static deflection used by Johnson *et al.* (2001) for the taut string model (where $\lambda^2 = 0$). The remaining shape functions are sine functions: $\phi_{j+1}(x) = \sin \pi j x$, $j=1, \dots, m-1$.

Substituting the shape functions into the nondimensional equation of motion (1) and simplifying results in the matrix equation $\mathbf{M}\ddot{\mathbf{q}} + \mathbf{C}\dot{\mathbf{q}} + \mathbf{K}\mathbf{q} = \mathbf{f} + \boldsymbol{\phi}F_d(t)$ with mass \mathbf{M} , damping \mathbf{C} , and stiffness \mathbf{K} matrices, where vector $\mathbf{q} = [q_j]$ contains the generalized displacements, $\mathbf{f} = [f_1 \ f_2 \ \dots \ f_m]^T$ is the externally applied load vector with $f_i = \int_0^1 f(x, t) \phi_i(x) dx$, and $\boldsymbol{\phi}$ is the damper load vector $\boldsymbol{\phi} = [\phi_1(x_d) \ \phi_2(x_d) \ \dots \ \phi_m(x_d)]^T = [1 \ \sin(\pi x_d) \ \dots \ \sin(\{m-1\}\pi x_d)]^T$.

The resulting model captures the salient features of a cable damper system much better than with sine terms alone. With just 11 terms (static deflection plus 10 sine terms), the first several natural frequencies, damping ratios, and mode shapes are more accurate than those computed with 100 sine terms alone. Convergence tests showed this to be true in the uncontrolled case, in the case with the optimal passive linear viscous damper, and with an active damper.

For control design, the system dynamics may be equivalently written in state-space form with state equation $\dot{\boldsymbol{\eta}} = \mathbf{A}\boldsymbol{\eta} + \mathbf{B}F_d(t) + \mathbf{G}\mathbf{f}$ and measurement equation $\mathbf{y} = \mathbf{C}_y\boldsymbol{\eta} + \mathbf{D}_yF_d(t) + \mathbf{H}_y\mathbf{f} + \mathbf{v}$, where $\boldsymbol{\eta} = [\mathbf{q}^T \ \dot{\mathbf{q}}^T]^T$ is the state vector, $\mathbf{y} = [w(x_d, t) \ \ddot{w}(x_d, t)]^T + \mathbf{v}$ is a vector of noisy sensor measurements (includes the displacement and acceleration at the damper location), and \mathbf{v} is a vector of stochastic sensor noise processes.

3 CONTROL OF CABLE VIBRATION

Three types of dampers are considered in this study. The damper of primary interest is a general semiactive device, one that may exert any required *dissipative* force. However, comparison with passive linear viscous dampers, similar to the oil dampers that have been installed in numerous cable-stayed bridges, is vital to demonstrate the improvements that may be gained with semiactive damping

technology. Additionally, comparison with active control devices is useful as they bound the achievable performance.

Note first that modal damping ratios provide a useful means of determining the effectiveness of linear damping strategies. However, using a semiactive damper introduces a nonlinearity into the combined system. Consequently, performance measures other than modal damping must be used for judging the efficacy of nonlinear damping strategies in comparison with linear (passive or active) dampers. The primary measure of damper performance considered herein is the square root of the mean square cable deflection integrated along the length of the cable, defined by

$$\sigma_d^2(t) = E\left[\int_0^1 v^2(x, t) dx\right] = E[\mathbf{q}^T(t)\mathbf{M}\mathbf{q}(t)] = \text{trace}\{\mathbf{M}^{1/2}E[\mathbf{q}(t)\mathbf{q}^T(t)]\mathbf{M}^{1/2}\} \quad (4)$$

where $\mathbf{M}^{1/2}$ is a square symmetric matrix such that $\mathbf{M}^{1/2}\mathbf{M}^{1/2} = \mathbf{M}$. The corresponding RMS cable velocity $\sigma_v^2(t)$ may be computed similarly from the generalized velocities. For stationary response to a stationary stochastic excitation, these performance measures become constant and not functions of time.

A *passive linear viscous damper* gives force proportional to the velocity at the damper location, i.e. $F_d(t) = -c_d\dot{w}(x_d, t)$, where c_d is a nondimensional damping constant and $\dot{w}(x_d, t)$ is the nondimensional velocity at the damper location: $\dot{w}(x_d, t) = \boldsymbol{\phi}^T\dot{\mathbf{q}} = [\mathbf{0}^T \quad \boldsymbol{\phi}^T]\boldsymbol{\eta}$. The modal damping may be determined via a straightforward eigenvalue analysis. Note that the optimal passive damper supplies pure damping; stiffness tends to degrade the damper performance (Sulekh, 1990).

A controller for an ideal *active damper* is designed here by examining a family of H_2/LQG control designs, which were seen to perform well for cables without sag (Johnson *et al.*, 2001). These controllers use force proportional to an estimate of the state of the system, $F_d^{\text{active}}(t) = -\mathbf{L}\hat{\boldsymbol{\eta}}$, where $\mathbf{L} = \mathbf{R}^{-1}\mathbf{B}^T\mathbf{P}$ is the feedback gain that minimizes the cost function

$$J = \frac{1}{2}(\sigma_d^2 + \sigma_v^2) + R\sigma_{\text{force}}^2 = \lim_{T \rightarrow \infty} E\left[\frac{1}{T}\int_0^T \left(\frac{1}{2}\mathbf{q}^T\mathbf{M}\mathbf{q} + \frac{1}{2}\dot{\mathbf{q}}^T\mathbf{M}\dot{\mathbf{q}} + R F_d^2\right) dt\right] \quad (5)$$

where \mathbf{P} satisfies the algebraic Riccati equation $\mathbf{A}^T\mathbf{P} + \mathbf{P}\mathbf{A} - \mathbf{P}\mathbf{B}\mathbf{R}^{-1}\mathbf{B}^T\mathbf{P} + \mathbf{Q} = \mathbf{0}$ and \mathbf{Q} is a 2-block by 2-block diagonal matrix with $\frac{1}{2}\mathbf{M}$ on the diagonal blocks and $\mathbf{0}$ off diagonal. A standard Kalman filter observer is used to estimate the states of the system. By varying the control weight R , a family of controllers that use varying force levels can be designed.

Unlike an active device, a *smart damper*, such as a variable-orifice viscous damper, a controllable friction damper, or a controllable fluid damper (Spencer and Sain, 1997; Housner *et al.*, 1997), can only exert *dissipative* forces. Herein, a generic semiactive device model is assumed that is purely dissipative. Essentially, this requirement dictates that the force exerted by the damper and the velocity across the damper must be of opposite sign; i.e. $F_d(t)\dot{w}(x_d, t)$ must be less than zero. Figure 3 shows this constraint graphically.

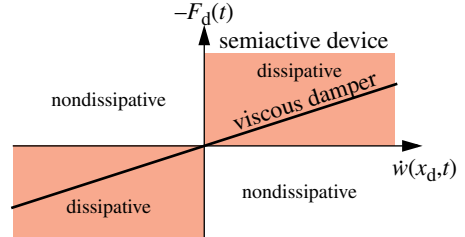


Figure 3. Smart damper dissipative forces.

A clipped optimal strategy is used, with a primary controller based on the same family of H_2/LQG designs used for the active damper, and a secondary controller to account for the nonlinear nature of the semiactive device. Here, the secondary controller simply clips non-dissipative commands using the function

$$F_d(t) = \begin{cases} F_d^{\text{active}}(t), & F_d^{\text{active}}(t)\dot{w}(x_d, t) < 0 \\ 0, & \text{otherwise} \end{cases} \quad (6)$$

4 EFFICACY OF SMART DAMPING STRATEGIES

There are no well established models for rain-wind induced galloping, though it tends to be dominated by the first few modes. The cable/damper system is here simulated with a stationary Gaussian white noise excitation shaped by the first mode of the cable with no sag (i.e. a half-sine). Without a

supplemental damper, and in the absence of sag, this half-sine excitation would energize just the first mode of the cable. A range of damper location and λ^2 are studied herein. The cable is assumed to have virtually no inherent damping without the supplemental damper, about 0.005% in the first mode. RMS responses to the excitation are computed via a Lyapunov solution for linear (passive and active) strategies and from simulation for smart dampers. A 1% RMS sensor noise corrupts each sensor measurement (modelled as Gaussian pulse processes).

The RMS cable displacement, defined in (4), as well as the RMS cable velocity and RMS damper force, were computed using a Lyapunov solution for passive and active control strategies, but through simulation for the smart damping system. Due to minimal damping in less aggressive control strategies and the resulting computation time considerations, only several semi-active controllers in the family of possible controllers are simulated here. The responses with the smart damper are shown using large bold markers (the same markers as the active and passive for a given value of the independent parameter λ^2). Figure 4 shows the RMS cable displacement as a function of the RMS damper force for a damper at $x_d = 0.02$ at several levels of sag. For strategies using small forces, the passive and active are nearly the same — this was also seen in Johnson *et al.* (2001) where similar was also observed about the semi-active strategy as well. However, at some point the passive damper begins to have diminished gains in spite of larger damper forces. This is due to the damper only “knowing” local information, that is, the cable velocity at the damper location. Effectively, the passive damper starts to lock the cable down at that point — certainly limiting the cable motion at the damper location — but allowing the rest of the cable to vibrate nearly unimpeded. The active and smart damping strategies, however, are able to take advantage of larger force levels in such a way that they do not lock the cable down, but rather continue to dissipate energy. The effect is that the controllable smart damper is able to achieve a 50 to 80 percent displacement reduction, depending on the sag, compared to the optimal passive linear viscous damper.

Figure 5 shows the RMS cable displacement for the three damping strategies versus the independent parameter λ^2 . Without sag ($\lambda^2 = 0$), the smart damper can provide about a 71% response decrease

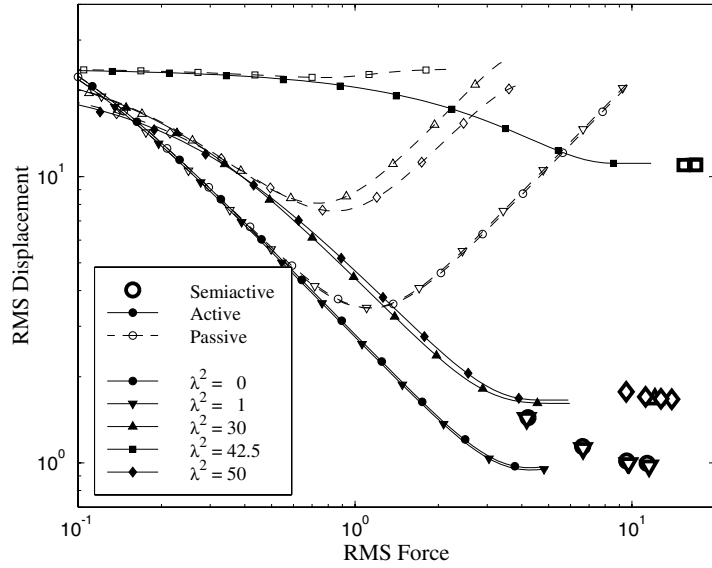


Figure 4. RMS displacement for a semiactive, passive viscous, or active dampers at $x_d = 0.02$ as a function of the RMS force.

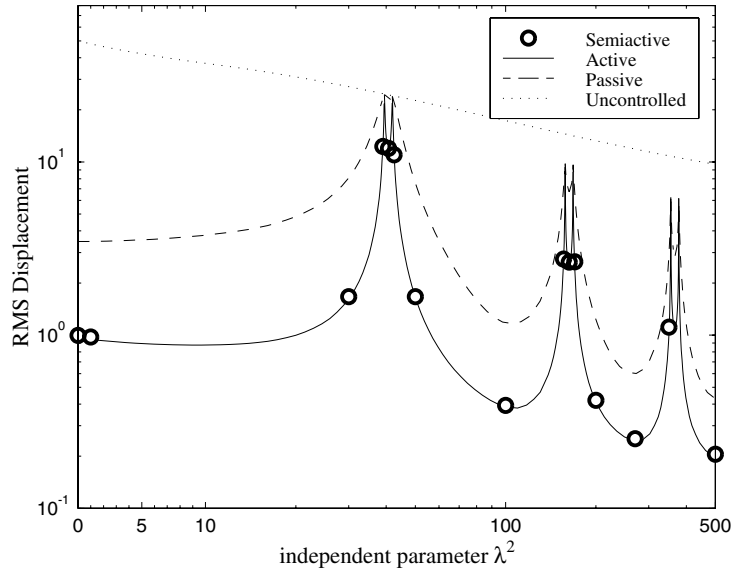


Figure 5. Minimum RMS displacement for smart, passive viscous, or active dampers at $x_d = 0.02$.

compared to the best passive device for $x_d = 0.02$. With small sag ($\lambda^2 = 1$), the RMS displacements decrease minutely for all three damping strategies. The smart damper always decreases response compared to the best passive damper, by 60 to 80 percent in most regions. Note, however, that the benefit comes with larger damper forces, though these force levels (Johnson *et al.*, 2001) are still well within the capabilities of current damper technology.

Increasing λ^2 , the performance degrades somewhat, and there are certain regions where all methods are ineffective. Figure 6 provides a closer look at the region of decreased performance around $\lambda^2 = 40$; it consists of two peaks of lousy performance with a valley of mediocre performance. The pairing of these two peaks is found for each of the three regions of decreased performance in the $[0, 500]$ range of λ^2 values studied here. The peaks of poor performance occur in pairs at λ^2 values of $(4\pi^2, 41.93)$, $(16\pi^2, 167.79)$, and $(36\pi^2, 377.59)$.

The RMS displacement with the active and smart damping strategies, relative to that of the optimal passive linear viscous damper, are shown in Figure 7 for a range of damper locations. Even for damper locations very near the cable support, smart damping can provide increased performance for various levels of sag. For damper locations around $x_d = 0.05$, the response with a smart damper is 55% to 70% less than with the passive damper. For most levels of sag, the superior relative performance only gets better for a damper closer to the end of the cable.

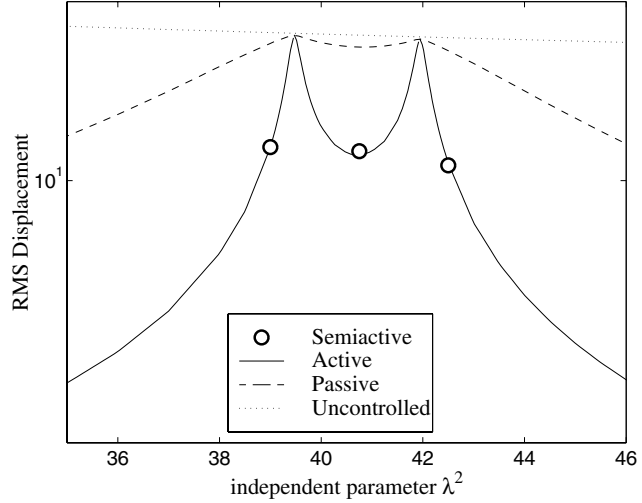


Figure 6. Minimum RMS displacement expanded views near three pairs of peaks ($x_d = 0.02$).

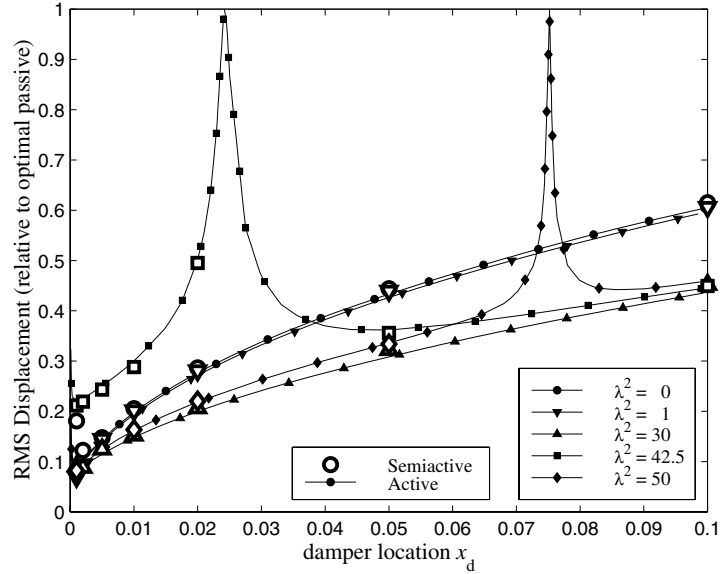


Figure 7. RMS displacement, relative to the optimal passive linear damper, with an active or smart damper at various damper locations.

5 DISCUSSION: THE EFFECTS OF SAG AND λ^2 ON CABLE MODES

The regions of poor performance by all three damping strategies are due to specific changes in the underlying dynamics of the cable alone. In the absence of a supplemental damper, the mode shapes of the cable without sag ($\lambda^2 = 0$) are sine functions, with integer natural frequencies. However, as the independent parameter λ^2 increases, the mode shapes that are symmetric about the center of the cable change significantly, while the antisymmetric mode shapes remain the same. These effects are discussed in depth elsewhere (e.g. Irvine, 1981). Figure 8 shows the first six natural frequencies of a sag cable as a function of the independent parameter λ^2 . Note particularly that due to the increased

stiffness on the symmetric modes, there are a number of frequency crossover points, where two modes have identical natural frequencies. These crossovers occur at $\lambda^2 = 4\pi^2$, $16\pi^2$, $36\pi^2$, etc. — that is, at $\lambda^2 = (2i\pi)^2$, $i = 1, 2, 3, \dots$ (Irvine, 1981). At these points, passive, active, and smart damper difficulties may be expected, since the manifold defined by the two modes with identical frequency can have controllable and uncontrollable subspaces with respect to a single point-located damping device. Indeed, the addition of any damping force will cause the motion of the cable to shift such that a node will occur at the damper location, with no possibility of adding damping to that mode.

Ill-conditioning also occurs when a mode has a node at the damper location. With sag, it is possible for the first several symmetric modes to have a node at a typical damper location. Figure 9 shows the first six mode shapes for ten values of λ^2 . Consider the thick line representing the first symmetric mode of the cable. At small λ^2 , it is sinusoidal in shape, but the slope at the ends flattens out with increasing sag. At $\lambda^2 = 4\pi^2$, the end slope is zero, as may be seen in the expanded view in Figure 10. As λ^2 increases beyond $4\pi^2$, the first symmetric mode has a node near each end of the cable. When λ^2 reaches 41.93, the node is at $x = 0.02$; a damper placed at $x_d = 0.02$ would be unable to control the first mode in this case.

Thus, the two phenomena of frequency crossover and nodes at the damper location explain the poor performance with all control strategies for particular values of λ^2 . Nevertheless, for most levels of sag, inclination, and longitudinal flexibility, a smart damper can reduce cable vibration significantly compared to the optimal passive linear damper.

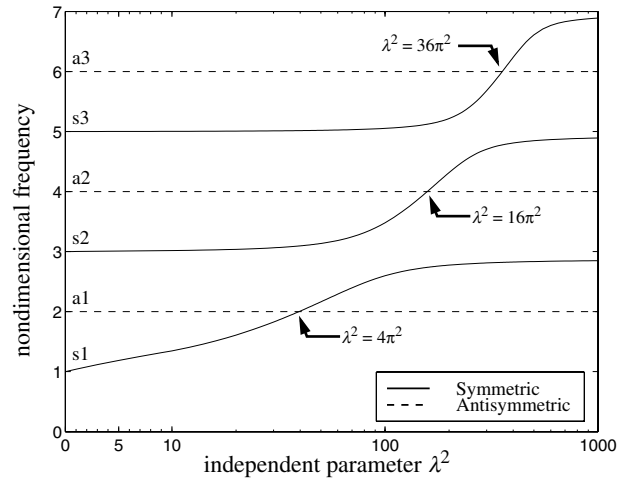


Figure 8. Natural frequencies as a function of the independent parameter λ^2 for sag cables.

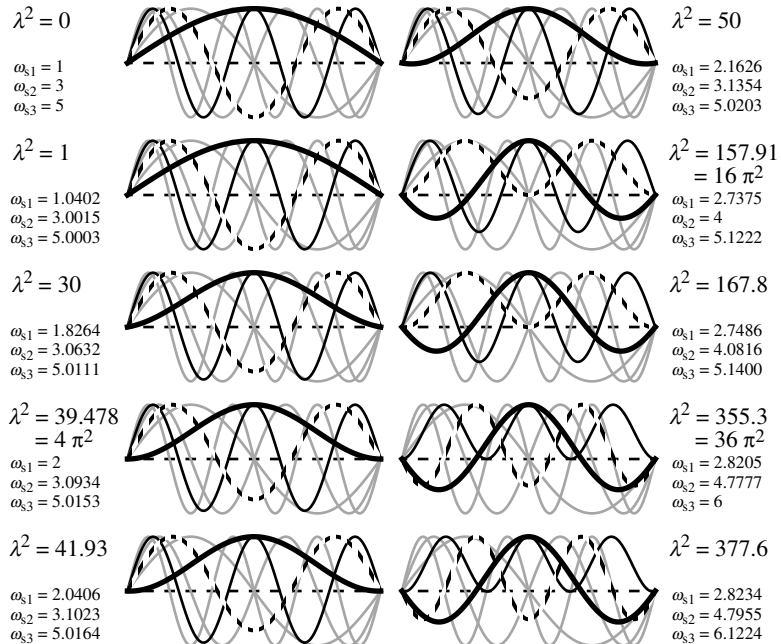


Figure 9. Cable mode shapes at various sag levels.

The antisymmetric modes are shown in gray. The natural frequencies (in nondimensional rads/sec) are given for the symmetric modes.

See also http://rcf.usc.edu/~johnsone/animations/cable_sag/.

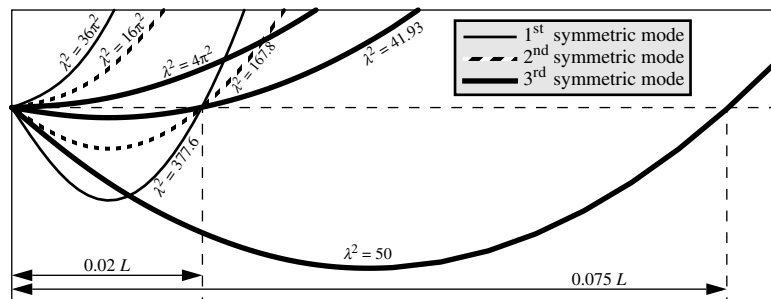


Figure 10. Expanded view of some cable mode shapes.

6 CONCLUSIONS

This paper extends a previous study by the authors on “smart” semiactive damping of stay cables. The previous study (Johnson *et al.*, 2001) showed that significant response reductions are available using smart dampers compared to the passive dampers currently in use for mitigating stay cable vibration. Herein, the effects of cable sag, inclination, and longitudinal flexibility have been introduced into the dynamic model of transverse in-plane cable vibration. A new low-order control-oriented model was developed to capture the salient dynamics of the cable/damper system. The performance of passive, active, and smart damper strategies are all found to degrade for certain combinations of damper location and independent parameter λ^2 that cause cable natural frequencies to coincide or that cause a node to occur at the damper location. When such a case occurs, the three damping strategies perform no better than the cable alone. However, for the general case, smart dampers provide significantly improved damping compared to the optimal passive viscous damper. Approximately 50 to 80 percent reduction in RMS response can be achieved compared to the optimal passive linear damper. The cost of this improvement is larger force levels — approximately 8–10 times larger for damper locations around $x_d = 0.02$. For the zero-sag case, Baker (1999) and Johnson *et al.* (2001) found that the peak force level during rain-wind induced motion of an example stay cable is on the order of 14 kN (3 kips) for a smart damper at $x_d = 0.01$. Thus, these larger forces are well within the cost-effective range of smart damping devices such as magnetorheological dampers. Consequently, smart dampers may be an effective replacement for passive viscous damping of cables.

ACKNOWLEDGEMENTS

The authors gratefully acknowledge the support of this research by the National Science Foundation under grant CMS 99-00234 and the LORD Corporation.

REFERENCES

- Baker, G.A. 1999. *Modeling and Semiactive Damping of Stay Cables*. Master’s Thesis, Department of Civil Engineering and Geological Sciences, University of Notre Dame.
- Gimsing, N.J. 1983. *Cable-Supported Bridges*, John Wiley & Sons, Chichester, England.
- Housner, G.W., L.A. Bergman, T.K. Caughey, A.G. Chassiakos, R.O. Claus, S.F. Masri, R.E. Skelton, T.T. Soong, B.F. Spencer, Jr., and J.T.P. Yao. 1997. Structural Control: Past and Present. *Journal of Engineering Mechanics*, ASCE. 123(9):897–971.
- Irvine, H.M. 1981. *Cable Structures*, MIT Press, Cambridge, Massachusetts.
- Johnson, E.A., G.A. Baker, B.F. Spencer, Jr. and Y. Fujino. 2001. Semiactive Damping of Stay Cables, ASCE *Journal of Engineering Mechanics*, in press.
- Kovacs, I. 1982. Zur Frage der Seilschwingungen und der Seildämpfung. *Die Bautechnik*. 10:325–332.
- Krenk, S. 1999. Vibrations of a Taut Cable with an External Damper. Technical Report No. 622, September 1999, Danish Center for Applied Mathematics and Mechanics, Technical University of Denmark.
- Pacheco, B.M., Y. Fujino, and A. Sulekh. 1993. Estimation Curve for Modal Damping in Stay Cables with Viscous Damper. *Journal of Structural Engineering*, ASCE. 119(6):1961–1979.
- Spencer, B.F., Jr. and M.K. Sain. 1997. Controlling Buildings: A New Frontier in Feedback. *IEEE Control Systems Magazine*. 17(6):19–35.
- Sulekh, A. 1990. *Non-dimensionalized Curves for Modal Damping in Stay Cables with Viscous Dampers*, Master’s Thesis, Department of Civil Engineering, University of Tokyo, Tokyo, Japan.
- Tunstall, M.J. 1997. Wind-Induced Vibrations of Overhead Transmission Lines: An Overview. *Proceedings of the International Seminar on Cable Dynamics*, Tokyo, Japan, October 13, 1997, 13–26.
- Watson, S.C., and D. Stafford. 1988. Cables in Trouble. *Civil Engineering*, ASCE. 58(4):38–41.